A family with axonal sensorimotor polyneuropathy with *TUBB3* mutation

YOUNG BIN HONG[1], JA HYUN LEE[2], HYUNG JUN PARK[1], YU-RI CHOI[1], YOUNG SE HYUN[2], JI HOON PARK[2], HEASOO KOO[3], KI WHA CHUNG[2] and BYUNG-OK CHOI[1]

[1]Department of Neurology, Samsung Medical Center, Sungkyunkwan University School of Medicine, Seoul 135-710; [2]Department of Biological Science, Kongju National University, Gongju, South Chungcheong 314-701; [3]Department of Pathology, Ewha Womans University School of Medicine, Seoul 120-750, Republic of Korea

Received February 18, 2014; Accepted November 3, 2014

DOI: 10.3892/mmr.2014.3047

Abstract. Mutations in the β-tubulin isotype III (*TUBB3*) gene result in *TUBB3* syndrome that includes congenital fibrosis of the extraocular muscle type 3 (CFEOM3), intellectual impairments and/or an axonal sensorimotor neuropathy. In the present study, a *TUBB3* D417N mutation was identified in a family with axonal sensorimotor polyneuropathy by whole exome sequencing. The proband exhibited gait disturbance at the age of 12 years and was wheelchair bound at 40 years. However, the proband's cousin exhibited gait disabilities at 45 years of age and was still able to walk when he was 60 years old. Ophthalmoplegia and intellectual impairment were not observed in either patient. A sural nerve biopsy identified an absence of large myelinated fibers without demyelinating degeneration. Based on these clinical features, the two patients exhibited an axonal peripheral neuropathy without CFEOM3. These results therefore suggested that certain *TUBB3* mutations may predominantly be associated with axonal peripheral neuropathy. Furthermore, the results also suggested that *TUBB3* mutations may be implicated in modulating the inter- and intra-familial heterogeneity of clinical phenotypes.

Correspondence to: Dr Byung-Ok Choi, Department of Neurology, Samsung Medical Center, Sungkyunkwan University School of Medicine, 81 Irwon-Ro, Seoul, Gyeonggi 135-710, Republic of Korea
E-mail: bochoi@skku.edu

Dr Ki Wha Chung, Department of Biological Science, Kongju National University, 56 Gongjudaehak-ro, Gongju, South Chungcheong 314-701, Republic of Korea
E-mail: kwchung@kongju.ac.kr

Key words: axonal sensorimotor polyneuropathy, β-tubulin isotype III, congenital fibrosis of the extraocular muscle type 3, whole exome sequencing

Introduction

Heterozygous missense mutations in β-tubulin isotype III (*TUBB3*), which is exclusively expressed in neurons (1), result in the *TUBB3* syndrome, which includes congenital fibrosis of the extraocular muscle type 3 (CFEOM3), intellectual impairments, facial paralysis and/or an axonal sensorimotor neuropathy (2,3). These findings suggested that *TUBB3* has a role in mediating axon guidance and maturation (4,5). Brain magnetic resonance imaging (MRI) of patients with *TUBB3* mutations has demonstrated evidence of dysgenesis of the corpus callosum, anterior commissure and internal capsule as well as generalized loss of white matter (4). However, to the best of our knowledge, there has been no report evaluating the features of lower limb MRIs of patients with *TUBB3* mutations.

Patients in the same family who harbored the D417N mutation in *TUBB3* exhibited a broad clinical spectrum, including CFEOM3 only; mixed features of CFEOM3 with peripheral neuropathy, learning disabilities and developmental delay; peripheral neuropathy only or no clinical symptoms (3,4). Therefore, the *TUBB3* mutation may cause an isolated axonal sensorimotor polyneuropathy and detailed descriptions of the histopathology of sural nerve and lower extremity MRI results require further evaluation.

The present study evaluated individuals exhibiting an axonal sensorimotor polyneuropathy with the D417N mutation in *TUBB3,* which was identified by whole exome sequencing (WES), and reports the pathophysiological results observed.

Materials and methods

Patients. The present study enrolled five members of a Korean family which was severely affected by axonal Charcot-Marie-Tooth (CMT) (FC423), including two affected individuals. A healthy 45-year-old male was enrolled for nerve histology study. Written informed consent was obtained from all participants according to the protocol approved by the Institutional Review Board for Ewha Womans University, Mokdong Hospital (approval no. ECT 11-58-37; Seoul, Korea).

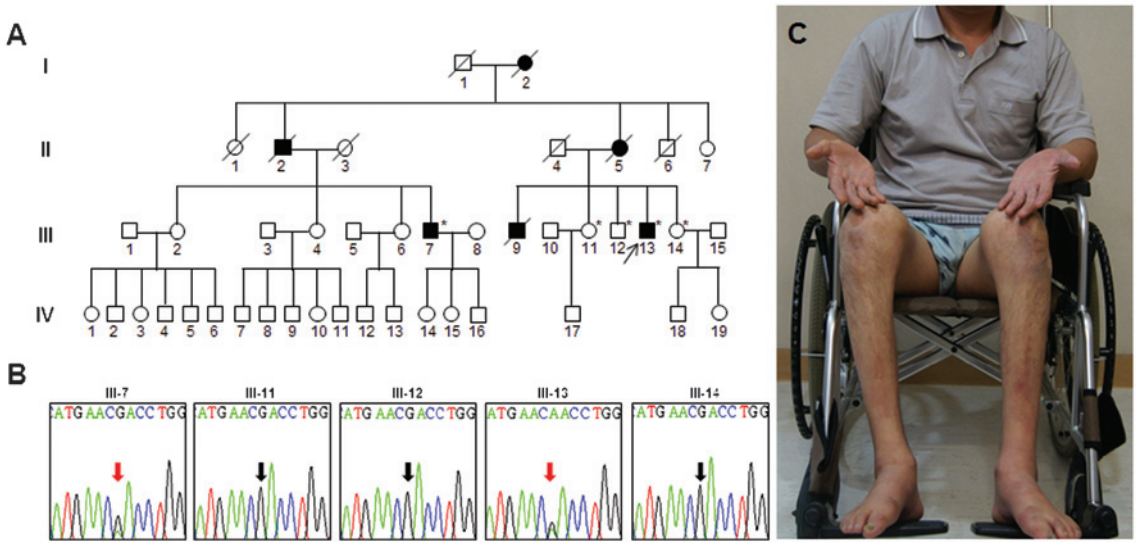

Figure 1. Pedigree, sequencing chromatograms and a clinical image. (A) Pedigree of the patients. The open and filled symbols represent unaffected and affected individuals, respectively. The proband is indicated by an arrow. Asterisks indicate the individuals whose DNA was used for capillary sequencing; symbols indicate the following: Square, male; round, symbol with line through, deceased. (B) Sequencing chromatograms for *TUBB3* mutations. Black and red arrows indicate the wild-type and mutation, respectively. (C) Image of the proband who was wheelchair-bound with marked atrophy of the lower leg muscles.

DNA preparation and whole exome sequencing. DNA from peripheral blood was isolated using a QIAamp blood DNA purification kit (Qiagen, Hilden, Germany). The isolated DNA was prescreened for duplication of 17p12 (PMP22) and mutations in the coding exons of GJB1, MPZ, NEFL and MFN2 as previously described (6). WES and subsequent filtering were performed in the affected members as previously described (7).

Capillary sequencing. Mutations in *TUBB3* were analyzed by capillary sequencing. Exon four, harboring the mutation site, was amplified using the following primers (Macrogen, Seoul, Korea): Forward, 5'-CATCCAGAGCAAGAACAGCA-3' and reverse, 5'-TTCGTACATCTCGCCCTCTT-3'. Polymerase chain reaction (PCR) amplifications was performed using Platinum PCR SuperMix High Fidelity kit (Life Technologies, Grand Island, NY, USA), with the above primers and the genomic DNA of the patients. Amplification was performed as follows: 32 cycles of 95˚C for 30 sec, 56˚C for 30 sec and 72˚C for 60 sec. Following amplification, the sequences were analyzed using a BigDye terminator cycle sequencing kit and automatic genetic analyzer (ABI3130XL; Applied Biosystems, Life Technologies, Foster City, CA, USA).

Clinical assessments. Clinical assessments were performed by two independent neurologists as previously described (8). Patients were evaluated by taking a comprehensive medical history, including details of motor and sensory impairments, deep tendon reflexes, muscle atrophy and gait abnormalities, for example walking on heels or toes. The muscle strength of the flexor and extensor muscles was measured manually using the Medical Research Council scale (http://www.mrc.ac.uk). In order to determine physical disability, three scales were used: The functional disability scale (FDS) (9), CMT neuropathy score (CMTNS) (10) and sensory impairment, which was assessed with regard to the level and severity of pain, temperature, vibration and position.

Electrophysiological examination. Electrophysiological studies were performed using the Sierra Wave EMG system (Cadwell Laboratories, Inc., Kennewick, WA, USA) and the Toennies two-channel NeuroScreen system (Jaeger-Toennies, Hochberg, Germany). Motor nerve conduction velocities (MNCVs) of the median and ulnar nerves were determined by electrical stimulation at the elbow or wrist, while recording compound muscle action potentials (CMAPs) over the abductor pollicis brevis and adductor digiti quinti, respectively. Similarly, the MNCVs of the peroneal and tibial nerves were determined by stimulation at the knee and ankle, while recording CMAPs over the extensor digitorum brevis and adductor hallucis, respectively. CMAP amplitudes were measured from baseline to negative peak values. Sensory nerve conduction velocities were measured over the finger-wrist segment from the median and ulnar nerves by orthodromic scoring, and were also recorded for sural nerves. Sensory nerve action potential (SNAP) amplitudes were measured from positive to negative peaks. An electromyography (EMG) was performed in the bilateral proximal and distal limb muscles.

Lower extremity MRI. MRI study of the proband was performed using the Siemens Vision 1.5-T system (Siemens, Erlangen, Germany). MRI was performed in the axial (field of view, 24-32 cm; slice thickness, 10 mm and slice gap, 0.5-1.0 mm) and coronal planes (field of view, 38-40 cm; slice thickness, 4-5 mm and slice gap, 0.5-1.0 mm) using the following protocol: T1-weighted spin-echo (SE) [repetition time (TR)/echo time (TE) 570-650/14-20; 512 matrixes], T2-weighted SE (TR/TE 2800-4000/96-99; 512 matrixes) and fat-suppressed T2-weighted SE (TR/TE 3090-4900/85-99; 512 matrixes).

Histopathological studies. Histopathological analysis of the distal sural nerve was performed on the proband. Semi-thin sections were stained with 0.1% Toluidine blue solution

Table I. Electrophysiological features of patients with the D417N mutation in the *TUBB3* gene.

Features	III-7		III-13		Normal value
Age at exam (years)	60		48		
Side	Right	Left	Right	Left	
Median nerve					
TL (ms)	**6.8**	**5.5**	**6.0**	**5.4**	<3.9
CMAP (mV)	**5.6**	6.9	**0.8**	**2.2**	>6.0
MNCV (m/s)	**39.1**	**40.6**	**39.7**	**39.7**	>50.5
Ulnar nerve					
TL (ms)	**4.4**	**3.8**	**3.6**	**3.7**	<3.0
CMAP (mV)	10.9	8.8	12.6	12.0	>8.0
MNCV (m/s)	**40.0**	**45.7**	**52.3**	**53.7**	>51.1
Peroneal nerve					
TL (ms)	**A**	**A**	**A**	**A**	<5.3
CMAP (mV)	**A**	**A**	**A**	**A**	>1.6
MNCV (m/s)	**A**	**A**	**A**	**A**	>41.2
Tibial nerve					
TL (ms)	**A**	**A**	**A**	**A**	<5.4
CMAP (mV)	**A**	**A**	**A**	**A**	>6.0
MNCV (m/s)	**A**	**A**	**A**	**A**	>41.1
Median sensory nerve					
SNAP (μV)	**A**	**A**	**A**	**A**	>8.8
SNCV (m/s)	**A**	**A**	**A**	**A**	>39.3
Ulnar sensory nerve					
SNAP (μV)	**A**	**A**	**A**	**A**	>7.9
SNCV (m/s)	**A**	**A**	**A**	**A**	>37.5
Sural nerve					
SNAP (μV)	**A**	**A**	**A**	**A**	>6.0
SNCV (m/s)	**A**	**A**	**A**	**A**	>32.1

Bold print denotes abnormal values. A, absent potentials; TL, terminal latency; CMAP, compound muscle action potential; MNCV, motor nerve conduction velocity; SNAP, sensory nerve action potential; and SNCV, sensory nerve conduction velocity.

(Sigma-Aldrich, St. Louis, MO, USA) for 3 min and then dehydrated with ethanol (Sigma-Aldrich). The density of myelinated fibers (MFs), axonal diameter and myelin thickness were determined using a computer-assisted image analyzer (AnalySIS 3.0; Soft Imaging System, Münster, Germany). Ultrathin sections were contrasted with uranyl acetate and lead citrate for ultrastructural study using a transmission electron microscope (H-7650; Hitachi, Tokyo, Japan).

Results

Genetic analysis. WES was performed in the two affected family members (Fig. 1A; III-7 and III-13). The total sequencing yields were 6.63 and 8.67 Gbp, respectively. Subsequent filtering identified 11 variants, which were shared by the affected family members (data not shown). Among the variants identified, the heterozygous D417N (c.1249G>A) mutation in *TUBB3* was shown to be a cause of CFEOM3 (4). Since patients harboring the same mutation exhibited peripheral neuropathy, it was concluded that the D417N mutation was the putative cause of the clinical features observed in the patients examined in the present study. Capillary sequencing confirmed that the mutation was co-segregated within the family members (Fig. 1B).

Clinical manifestations. The proband (Fig. 1A, III-13; 48 years old) initially exhibited gait disturbance at 12 years of age. Progressive gait impairment was identified and the proband became wheelchair bound at 40 years of age (Fig. 1C). At 48 years, significant muscle weakness and atrophy of the distal lower limbs was observed. All sensory modalities were severely impaired and the vibration sense was more markedly affected than the pinprick sense. Deep tendon reflexes were absent and pathological reflexes were not present in all limbs. However, the proband did not demonstrate ophthalmoplegia, blepharoptosis or strabismus (Fig. 2). Mini-mental state examination and all cranial nerve examinations were normal.

By contrast, a 60-year-old cousin of the proband (Fig. 1A; III-7) began to experience gait disabilities when he was

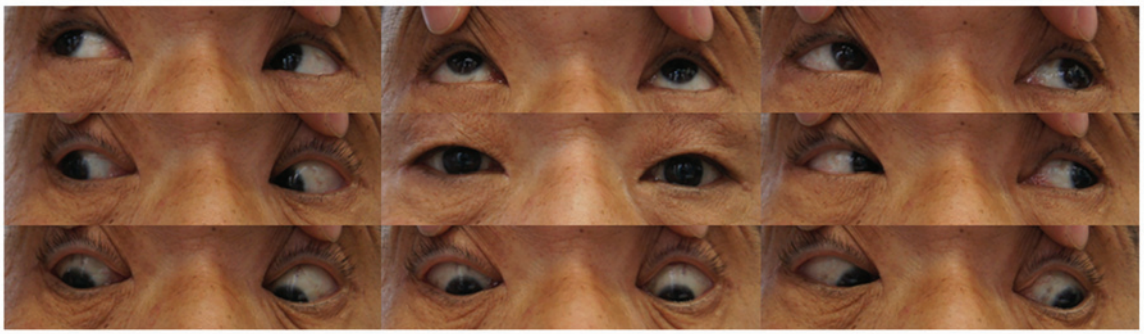

Figure 2. Normal extraocular movement of the proband. Ophthalomoplegia was not detected.

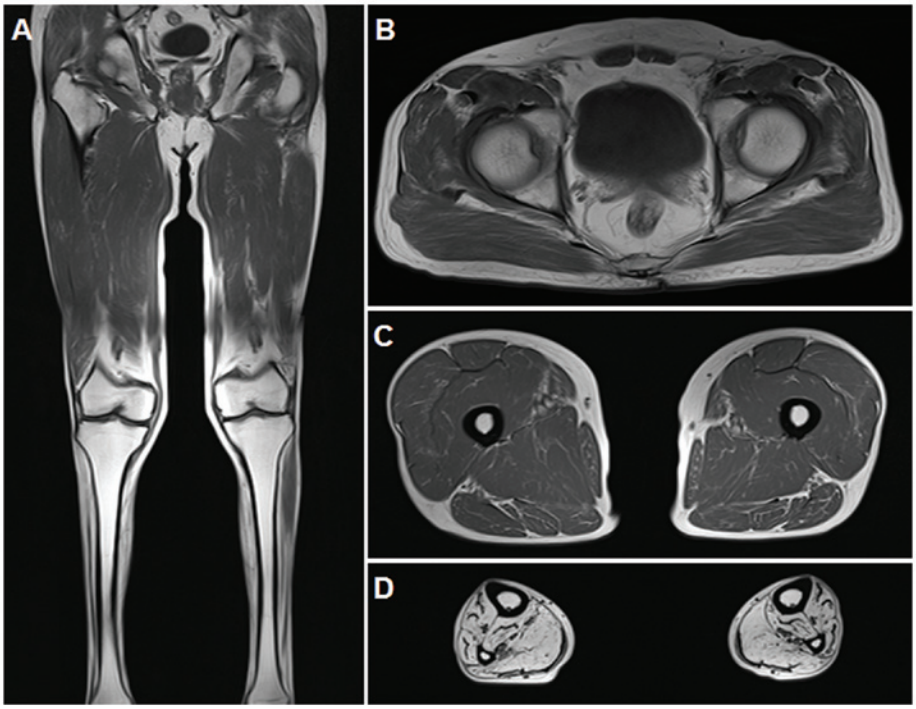

Figure 3. Lower extremity magnetic resonance image of the proband (III-13). (A) T1-weighted coronal image of the lower extremities indicated markedly hyperintense signal changes and atrophies in all muscles of the lower leg, whereas all muscles of the thigh and hip were normal. (B) T1-weighted axial images of the hip revealed normal characteristics. (C) At the thigh level, no muscles revealed fatty changes. (D) T1-weighted axial images of the calf indicated that almost all muscles demonstrated markedly diffuse atrophies and fatty hyperintense signal changes.

45 years old and, unlike the proband, was still able to walk using ankle-foot devices. Neurological examination at 60 years of age revealed bilateral pes cavus and distal muscle atrophy of the upper and lower limbs. Based on the medical history notes taken, the deceased family members (I-2, II-2, II-5 and III-9) had exhibited distal lower limb weakness and gait disturbance. Furthermore, none had experienced any eye symptoms.

Axonal neuropathies identified by electrophysiological analysis. Nerve conduction studies were performed on the two patients aged 48 and 60 years, respectively (Table I). The values of the median MNCV were from 39.1-40.6 m/s, and those of the ulnar MNCV were from 40.0-53.7 m/s. Right CMAPs of the median nerves were below normal range, whereas those of the ulnar nerve were normal. Tibial and peroneal MNCVs were not elicited and SNAPs of the median, ulnar and sural nerves were absent. A needle EMG identified fibrillation potentials, positive sharp waves and neurogenic motor unit action potentials.

Lower extremity MRI results are length-dependent. MRIs of the lower extremities of the proband revealed hyperintense signal abnormalities in the lower leg muscles (Fig. 3A), whereas brain MRIs exhibited normal features (data not shown). T1-weighted images identified marked muscle atrophy with signal alterations observed in the lower leg muscles compared to those of the hip and thigh muscles. The predominant atrophy of the distal muscles was consistent with the length-dependent neuropathy hypothesis. At the hip (Fig. 3B) and thigh (Fig. 3C) levels, the fatty involvement of compartment muscles was not observed. By contrast, almost all muscles in the lower extremities demonstrated diffuse atrophies and fatty hyperintense signal changes (Fig. 3D).

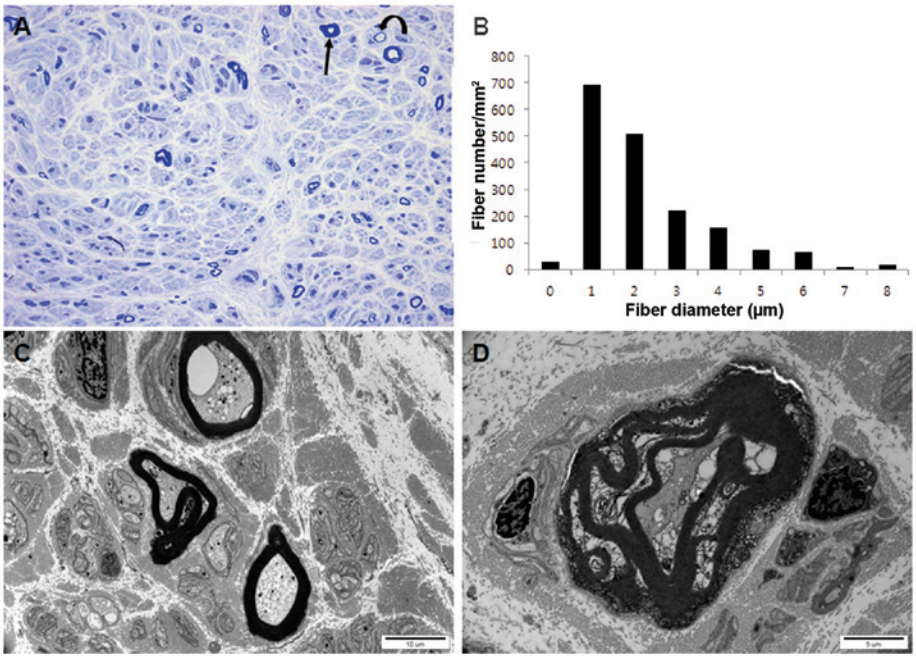

Figure 4. Histopathological characterization of distal sural nerve biopsy from the patient (III-13). (A) Toluidine blue-stained semi-thin transverse section analysis revealed an absence of large MFs (magnification, x400). The remaining medium- and small-sized MFs were widely scattered and thinly myelinated (curved arrow), and thick MFs were rarely identified (arrow). (B) Histogram demonstrating a unimodal distribution pattern. (C and D) Electron micrographs revealed myelinated and unmyelinated axons with vacuolization of the axoplasm and degenerating abnormal mitochondria. Scale bar, 10 μm for C and 5 μm for D. MFs, myelinated fibers.

Histopathological observations. Histopathological examination of the distal sural nerve of the proband (III-13) aged 48 years revealed an absence of large MFs, with the presence of small- or medium-sized and thinly scattered MFs (Fig. 4A). Regenerating axonal clusters and thick MFs were rarely identified. The number of remaining MFs (1,770/mm^2) was markedly lower than that of a healthy 45-year-old male volunteer (7,300/mm^2). The range and average MF diameter were smaller than age-matched controls and the histogram identified a unimodal distribution pattern (Fig. 4B). Electron microscopic examination revealed scattered myelinated and unmyelinated axons with swelling or vacuolization of the axoplasm as well as degenerated abnormal mitochondria and membranous structures (Fig. 4C). Degenerating MFs with the breakdown of myelin and axons were rarely noted (Fig. 4D). Although there were thinly scattered MFs, no further evidence of demyelination, including demyelinated axons or onion bulb formation, were present.

Discussion

The present study revealed that a Korean family with a *TUBB3* mutation exhibited an axonal sensorimotor neuropathy. Histopathological analysis of the sural nerve biopsy of the proband revealed features characteristic of an axonal neuropathy, including a decreased number of MFs, the absence of large MFs and abnormally thick MFs. However, CFEOM3, ophthalmoplegia and intellectual impairment were not observed in the two patients. According to previous studies, the clinical features of the D417N mutation in *TUBB3* are heterogeneous (4). Tischfield *et al* (4) compared the phenotypes of 15 individuals from four families harboring the mutation: Three patients exhibited CFEOM3 only, four patients exhibited CFEOM3 with peripheral neuropathy, two patients exhibited CFEOM3 with peripheral neuropathy and developmental delay, three patients exhibited peripheral neuropathy only, one patient exhibited CFEOM3 with peripheral neuropathy and learning disability, one patient exhibited CFEOM3 with learning disability and one patient was a non-penetrant carrier. Therefore, one-fifth of the patients exhibited a peripheral neuropathy phenotype only. An alternate amino acid change at the same site (D417H) also resulted in a heterogeneous phenotype within a family: All three affected family members exhibited CFEOM, wrist and finger contractures and facial weakness. However, one family member exhibited peripheral neuropathy, while another exhibited peripheral neuropathy with additional developmental delay and the third did not exhibit peripheral neuropathy (3). These results supported the hypothesis that mutations at the D417 position result in a broad phenotypic spectrum, suggesting that the clinical features may depend on the genetic background of each individual. In the present study, in comparison to the proband, his cousin experienced late-onset symptoms and a mild phenotype. Therefore, these patients exhibited clinical diversity within the family.

Application of WES was found to be a cost- and time-effective method used to reveal the underlying genetic causes of rare human diseases (11-13). Previous studies by our group have also applied WES and successfully isolated the causative mutations of patients with peripheral neuropathy (7,14-16). In the present study, the sole genetic cause of the symptoms observed was not isolated. However, certain evidence has suggested that the *TUBB3* mutation may be the underlying causative gene of CMT in the patients examined in the present study. Only the *TUBB3* D417N mutation has been reported to cause peripheral neuropathy and only four of those

genes (*APPL2, LMO7, TNRC6C* and *TUBB3*) were expressed in the sural nerve according to transcriptome sequencing (data not shown). The *TUBB3* D417N mutation was not found in the Korean controls (n=300) or reported in the Exome Variant Server (http://evs.gs.washington.edu/EVS/). Therefore, it was concluded that the *TUBB3* mutation was the genetic cause of the axonal neuropathy observed.

To the best of our knowledge, to date, pathological features in the sural nerve have not been reported in patients with *TUBB3* mutations. In the present study, a distal sural nerve biopsy was performed on a patient harboring a *TUBB3* mutation. The results identified marked axonal loss, but no other evidence of demyelination, including demyelinated axons or onion bulb formation, were present. In addition, the nerve conduction studies indicated that the median and ulnar nerve conduction velocities were >38 m/s, and electromyography revealed neurogenic motor unit action potentials and fibrillation potentials. These results were compatible with those expected in axonal neuropathy.

MRI analysis revealed a distinct pattern of muscular involvement, where markedly greater muscle atrophy with hyperintense signal changes was identified in the lower leg muscles than that in the thigh or hip muscles. This was compatible with the hypothesis of length-dependent axonal degeneration. Previously, a type-specific pattern of fatty infiltration in muscles was reported: In demyelinating hereditary motor and sensory neuropathy (HMSN type 1A) the tibialis anterior and peronei muscles were predominantly involved. However, late-onset axonal HMSN type 2A revealed predominant involvement of the soleus muscle, whereas early-onset HMSN type 2A exhibited whole calf and muscle involvements, including moderate to severe fatty changes in the thigh muscle (17). In the present study, the proband exhibited whole-compartment calf muscle involvement with no involvement of the thigh muscles. The proband therefore exhibited a pattern which differed from those identified in axonal HMSN type 2A. These findings are likely due to the variable pathophysiologies of axonal neuropathies.

In the future, specific molecular diagnoses will be important for the development of personalized therapies for axonal neuropathy. In this context, the results of the present study may aid in the development of genetic testing for axonal neuropathypatients.

Acknowledgements

The present study was supported in part by the Korean Health Technology R&D Project, Ministry of Health & Welfare (Sejong, Korea; no. A120182).

References

1. Katsetos CD, Legido A, Perentes E and Mörk SJ: Class III beta-tubulin isotype: a key cytoskeletal protein at the crossroads of developmental neurobiology and tumor neuropathology. J Child Neurol 18: 851-866, 2003.
2. Poirier K, Saillour Y, Bahi-Buisson N, *et al*: Mutations in the neuronal β-tubulin subunit *TUBB3* result in malformation of cortical development and neuronal migration defects. Hum Mol Genet 19: 4462-4473, 2010.
3. Demer JL, Clark RA, Tischfield MA and Engle EC: Evidence of an asymmetrical endophenotype in congenital fibrosis of extraocular muscles type 3 resulting from *TUBB3* mutations. Invest Ophthalmol Vis Sci 51: 4600-4611, 2010.
4. Tischfield MA, Baris HN, Wu C, *et al:* Human *TUBB3* mutations perturb microtubule dynamics, kinesin interactions, and axon guidance. Cell 140: 74-87, 2010.
5. Jiang YQ and Oblinger MM: Differential regulation of beta III and other tubulin genes during peripheral and central neuron development. J Cell Sci 103: 643-651, 1992.
6. Choi BO, Kim J, Lee KL, Yu JS, Hwang JH and Chung KW: Rapid diagnosis of CMT1A duplications and HNPP deletions by multiplex microsatellite PCR. Mol Cells 23: 39-48, 2007.
7. Choi BO, Koo SK, Park MH, *et al*: Exome sequencing is an efficient tool for genetic screening of Charcot-Marie-Tooth Disease. Hum Mutat 33: 1610-1615, 2012.
8. Chung KW, Hyun YS, Lee HJ, *et al*: Two recessive intermediate Charcot-Marie-Tooth patients with GDAP1 mutations. J Peripher Nerv Syst 16: 143-146, 2011.
9. Birouk N, LeGuern E, Maisonobe T, *et al*: X-linked Charcot-Marie-Tooth disease with connexin 32 mutations: clinical and electrophysiologic study. Neurology 50: 1074-1082, 1998.
10. Shy ME, Blake J, Krajewski K, *et al*: Reliability and validity of the CMT neuropathy score as a measure of disability. Neurology 64: 1209-1214, 2005.
11. Choi M, Scholl UI, Ji W, *et al*: Genetic diagnosis by whole exome capture and massively parallel DNA sequencing. Proc Natl Acad Sci USA 106: 19096-19101, 2009.
12. Bamshad MJ, Ng SB, Bigham AW, Tabor HK, Emond MJ, Nickerson DA and Shendure J: Exome sequencing as a tool for mendelian disease gene discovery. Nat Rev Genet 12: 745-755, 2011.
13. Ng SB, Buckingham KJ, Lee C, *et al*: Exome sequencing identifies the cause of a Mendelian disorder. Nat Genet 42: 30-35, 2010.
14. Lee SS, Lee HJ, Park JM, *et al*: Proximal dominant hereditary motor and sensory neuropathy with proximal dominance association with mutation in the TRK-fused gene. JAMA Neurol 70: 607-615, 2013.
15. Nakhro K, Park JM, Hong YB, *et al*: SET binding factor 1 (SBF1) mutation causes Charcot-Marie-Tooth disease type 4B3. Neurology 81: 165-173, 2013.
16. Kim HJ, Hong YB, Park JM, *et al*: Mutations in the PLEKHG5 gene is relevant with autosomal recessive intermediate Charcot-Marie-Tooth disease. Orphanet J Rare Dis 8: 104, 2013.
17. Chung KW, Suh BC, Shy ME, *et al*: Different clinical and magnetic resonance imaging features between Charcot-Marie-Tooth disease type 1A and 2A. Neuromuscul Disord 18:610-618, 2008.